

## Drop tower impact rig to assess the effectiveness of suspension seat for small high-speed passenger craft



Faisal Ikram Bin Abd Samad<sup>1,2\*</sup>, Mohd Yuzri Bin Mohd Yusop<sup>2</sup>, Nik Mohd Ridzuan Bin Shaharuddin<sup>1,3</sup>, Omar Bin Yaakob<sup>1,3</sup>

<sup>1</sup>School of Mechanical Engineering, Faculty of Engineering, Universiti Teknologi Malaysia, Skudai, Johor, Malaysia

<sup>2</sup>Universiti Kuala Lumpur, Malaysian Institute of Marine Engineering Technology, Lumut, Perak, Malaysia

<sup>3</sup>Marine Technology Centre, Universiti Teknologi Malaysia, Skudai, Johor, Malaysia

### ARTICLE INFO

#### Keywords:

Drop test

Suspension seat

High-speed craft

DRI

### ABSTRACT

This work aims to design a drop tower impact rig to examine the effectiveness of suspension seats for small high-speed passenger crafts and to evaluate whether the designed suspension seat can effectively mitigate the slamming impact on passengers and lower the risk of injuries. A drop tower was fabricated, and drop tests were conducted at different drop heights to simulate base impact acceleration between the range of 3g to 7g. Acceleration data captured using accelerometers were low pass filtered accordingly, and the seat effectiveness and safety were analyzed using the Dynamic Response Index (DRI). The seat's stiffness was experimentally and theoretically analyzed using Hooke's Law, and damping values were analyzed using the logarithmic decrement method. The results revealed that DRI values, limited to 18, can only be attained with deck acceleration of less than 6.73g. The tested suspension seat reduced the impact severity by 54 %. This impact mitigation is achievable with an underdamped system of average stiffness and damping rates of 64.8 kN/m and 211 Ns/m, respectively. The research has successfully proved that the fabricated drop tower could simulate the base impact acceleration of desired slamming impact acceleration according to drop heights and that the designed suspension seat can mitigate the severity of the slamming impact effectively.

### 1. Introduction

A suspension seat is one method to mitigate the slamming impacts on passengers onboard high-speed crafts (HSC). The use of suspension seats is common to navies and coastguards on their rescue and patrol crafts. The requirements for them to operate in high speed and rough sea conditions may lead them to experience large slamming impacts, which puts their safety and health at risk. Lower back and neck fractures are the most common injuries reported from these excessive impacts [1, 2]. Vertical accelerations from slamming impacts might also impair the ability of the crew to carry out their duties [3-5]. Besides injuring the occupants, a slamming impact, even short in duration [6], can significantly damage a marine structure, causing global whipping responses, local transient vibrations [7], and dynamic instabilities [8, 9]. The International

\* Corresponding author.

E-mail address: [faisalikram@unikl.edu.my](mailto:faisalikram@unikl.edu.my)

Code of Safety for High-Speed Craft [10] has set a limit of 1g for vertical accelerations due to slamming impacts at the longitudinal centre of gravity of the craft.

The effectiveness of suspension seats can be measured using various models and standards provided by several international organizations. For example, the Vibration Dose Value (VDV) provided by the British Standards Institute (BSI) under the BS 6841:1987 standard, Motion Sickness Dose Value (MSDVZ) and Maximum Transient Vibration Value (MTVV) under ISO 2631 -1: 1997 standard and Static Compression Dose (Sed) under ISO 2631 – 5: 2004 standard. Other organizations working on the same standards are the European Committee for Standardization (CEN), the Japanese Industrial Standards Committee (JISC), Deutsches Institut für Normung, Germany (DIN), and the American National Standards Institute (ANSI). In addition, there are other statistical methods, such as the Impact Count Index (ICI) [11] and the Most Probable Largest (MPL) [12] value of acceleration. In this research, the Dynamic Response Index (DRI) is used to analyze the effectiveness of the suspension seat. P.R. Payne developed the Dynamic Response Index (DRI) in the 1970s under the U.S. Air Force to assess potential injury for humans in a seated position [13]. This standard can relate the probability of injury to the human spine in the seated position from the obtained DRI values. The efficiency of the suspension seat to mitigate the shock is then measured directly through some number of gs (impact acceleration) that have successfully been reduced from the input source, in this case, the deck acceleration. This standard is discussed further in section 2.7 of this paper.

To demonstrate the effectiveness of the suspension seats, experimental test procedures have been carried out by other researchers, including laboratory tests [14, 15] and sea trial tests [12, 16, 17]. Accurate results can be obtained from sea testing, but difficulties arise from such an approach concerning repeatability, workforce, and time consumption. Drop tests in the laboratory offer an excellent alternative to replicate repeated slam loading and the associated force to the base of the suspension seat. The amount of acceleration experienced by HSC can be easily simulated by the drop height, which is proportional to the square root of the drop height and the inverse of the pulse width, which can be easily achieved by varying the floor material type (density, hardness, and geometry) to which the seat base carriage is dropped upon. Such testing procedure using a drop tower to test the effectiveness of suspension seats for HSC has been conducted at Carleton University's Applied Dynamics Laboratory (ADL) in collaboration with Defense Research and Development Canada-Atlantic (DRDC Atlantic) [15]. Two renowned brands of suspension seats in the HSC community were tested: The Shockwave Marine Suspension seat and the Ullman Dynamics Compact seat. A frequency-domain post-processing method based on the Eigensystem Realization Algorithm (ERA) was used to obtain the system parameters. Another method, an inexpensive drop table similar to the drop tower testing approach, was developed and conducted at the Massachusetts Institute of Technology (MIT) [18]. The objective was to develop and investigate testing methodologies and mitigating mechanical shocks on HSC. The suspension seat brand and model STIDD800v5 used on the US Navy boat was used for the testing. One famous HSC suspension seat brand, SHOXS, also adopted the same testing technique [19].

Besides the drop tower, the shaker table, such as that used at Virginia Polytechnic Institute [11], is another method to simulate slam load conditions for suspension seat tests. Compared to the drop tower, which can only simulate a single impulsive force, the shaker table can simulate multiple input forces from its continuously moving platform. For example, sinusoidal and square wave input signals can be programmed into the feedback control system, which then controls the actuator force, which moves and gives forces to the moving platform. However, this method is expensive and suitable for active or semi-active suspension systems.

Another testing machine with more advanced features was also developed at Carleton University. The testing machine is electronically controlled to produce large-amplitude motions of freefall slam impact, and the seat can be dropped onto electro-rheological dampers to obtain tunable response forces. The motions of a suspension seat can be controlled in two directions, simulating the heave and sway motions [20, 21]. Instead of fabricating a drop tower, the United Kingdom's Ministry of Defense (MOD) prepared a test standard (Protocol 1 2014) [22] for testing suspension seats by dropping an asymmetrical wedge onto a box of sand. An asymmetrical wedge is attached under a base platform and acts as a pulse shaper. Motivated by the test protocol conducted by the UK's MOD, a series of tests have been performed at Old Dominion University to

gather the relationship and effects of acceleration amplitude and duration at different wedge angles and drop heights [23]. The test fixture consists of the tested seat being dropped from the hook of a bridge crane using a quick-release mechanism activated by pulling a rope.

Driven by the above research projects, a drop tower was designed and fabricated at Universiti Kuala Lumpur, Malaysian Institute of Marine Engineering Technology (UniKL-MIMET) as part of its collaboration with Marine Technology Centre, Universiti Teknologi Malaysia (MTC-UTM) to assess the effectiveness of the constructed seat that is explicitly designed to be used on small high-speed passenger craft as shown in Fig. 1. These types of crafts are commonly used as means of transportation, as well as for fishing and conducting leisure activities. There are many brands and types of suspension seats available in the market. However, they are relatively expensive, and not all designs are suitable for installation on small high-speed passenger crafts, as shown in Fig. 1.



**Fig. 1** Small HSC, 7.9 meters in length [24]

The primary objective of this research is to design and fabricate an effective, low-cost suspension seat to be used onboard small, high-speed passenger craft. To investigate and validate its effectiveness, a drop tower was designed and fabricated. The drop tests were carried out to analyze its mitigation ability to a range of impact severity. A sea trial has been conducted on this craft to assess and analyze slamming impact accelerations. The highest acceleration recorded was 4.22g [24]. The expectation from this research is that the drop test procedure can demonstrate the effectiveness of slam shock mitigation and that the fabricated seat can reduce the impact of slam shock.

## 2. Drop testing and suspension seat

From the literature, the drop test procedure has proved its ability to simulate a single impulsive force as input for suspension seat base acceleration. The reproduction of slamming shock events experienced by HSC can be repeated and controlled. Unlike marine suspension seats, drop tests have been used in many areas, such as aircraft crashworthiness tests. Many research works implementing drop tests have been conducted in aviation technology to analyze the strength and impact-absorbing ability, especially at the fuselage and passenger area sections. A study that employs drop testing is actively carried out at NASA Langley Research Center, United States, and one of their recent tests was conducted on two full-scale Fokker F28 MK4000 aircraft sections to investigate the crashworthiness characteristics. In addition to the test, ten Anthropomorphic Test Devices (ATD) were included to measure the potential response of occupant injury [25].

In many cases, suspension seats can reduce the shock impact peaks due to slamming between 39.4 % and 64.2 % [26]. However, in some cases, the seat cushion can amplify the shock loads, and this could happen to overly compliant cushions that cause the occupant mass to move out of phase from the movement of the seat suspension [14, 22]. The suspension system, which consists of a spring-damper assembly, is also employed on land vehicles. Nevertheless, dynamic environments are different, and seats designed for the land vehicle may not be suitable for wave impact characteristics experienced on small HSCs. Thus, the correct suspension seat parameters according to craft types and operations criteria must be chosen carefully. A

laboratory test can demonstrate the mitigation performance of the suspension seat before its installation on HSC to ensure the seat can give enough protection to the occupant from harmful slam shocks.

### 2.1 The drop tower rig

The drop tower was fabricated at UniKL-MIMET, as shown in Fig. 2. The drop tower was fabricated using a "C" channel steel beam (75mm x 40mm x 5mm) and angle steel bar (25 mm x 25 mm x 3 mm) welded on both sides of the "C" channel which act as a guide rail for the vertical motion. The carriage assembly (where its base is used to secure the suspension seat for drop test) is attached to the "C" channel section using two roller bearings, which also act as a glider to allow motion only in the vertical directions as shown in Fig. 3. The "C" channel is bolted to its foundation plate (450 mm x 600 mm) using a 40mm thick steel plate that is heavy and sufficient to stabilize the structure and secured by three gusset plates on both sides of the beam to avoid lateral motions. Four legs with a length of 600 mm are bolted diagonally at the foundation base plate vertices of the structure to provide more stability and safety.

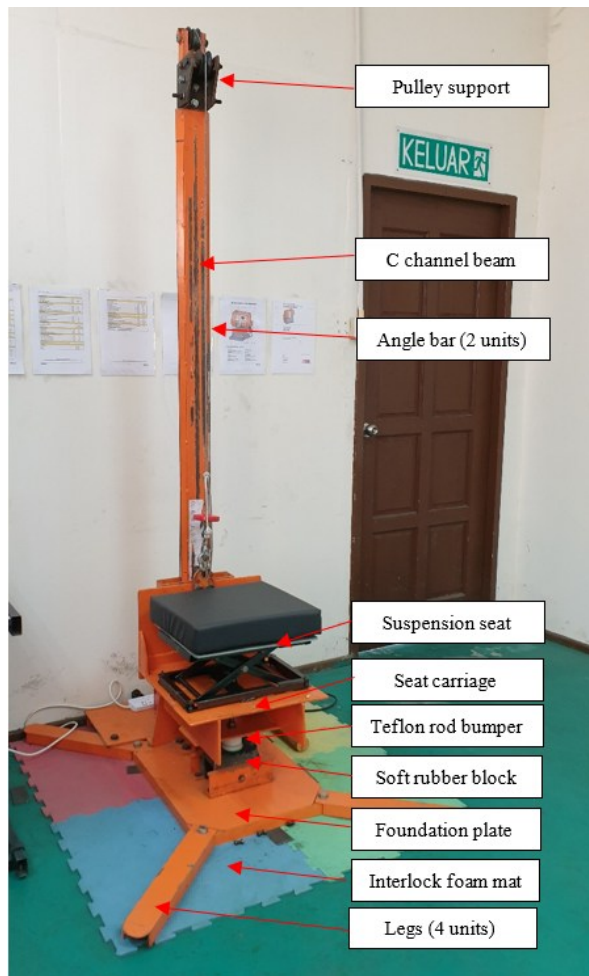


**Fig. 2** UniKL UTM drop tower



**Fig. 3** Roller bearing (2 units) attached to the angle bar (25 mm x 25 mm x 2 units)

To lift the carriage (450 mm x 450 mm x 10 mm) vertically up, which carries the seat and load plates, an electric clutch winch with a capacity of 600 kg is equipped and bolted on the tower base behind the "C" channel beam. Two steel roller bearings are installed at the top end of the "C" channel beam to complete the lifting pulley system. A manual, quick-release hook lets the carriage fall freely onto the impacting surface. A variable impacting surface is made of a soft rubber block and can be changed to obtain the desired pulse duration of the impact. Lastly, interlocking foam mats are placed below the drop tower to reduce the impact directed to the concrete floor. The drop test rig is designed with simplicity and cost-effectiveness in mind. Despite its straightforward design, it is highly capable of replicating impacts, which is critical for assessing the effectiveness of suspension seats.

## 2.2 Design requirement and fabrication of suspension seat

The designed seat will be installed on a small HSC with an average operating speed between 20 to 30 knots, depending on sea surface conditions. As small businesses commonly operate the craft, the aim is to produce a low-cost, lightweight, and retrofittable suspension seat that is effective enough to mitigate the slamming impact on passengers and lower their risks of injury.

Fig. 4 shows the prototype seat to be used on a small HSC, which is used in the drop test of this research paper. The seat frame is made from low-carbon steel, and the total weight is 9.3 kg. The seat legs are designed to work through a scissor mechanism, thus allowing it to move vertically. One side of the legs is fixed, and the other one can move freely, as shown in Fig. 5. A single shock absorber is mounted at the seat's center, connecting the seat's lower and upper parts, as shown in Fig. 6. Suction cups secure the seat on the boat's deck or existing fixed seats. According to the manufacturer, each suction cup can support weights of up to 250 N vertically, thus making the total force that the seat can withstand 1000 N. The holding strengths of the suction cups are even better when positioned on a flat horizontal surface.



**Fig. 4** Retrofittable lightweight prototype suspension seat



**Fig. 5** Replaceable Teflon inside a guide rail of the designed suspension seat



**Fig. 6** Attachment of shock absorber

## 2.3 Mathematical model of suspension seat

Fig. 7 illustrates the complete model of two-degree-of-freedom mechanical systems, showing the displacements of occupant mass and seat-pan mass. Equations (1) and (2) give the equations of motion.

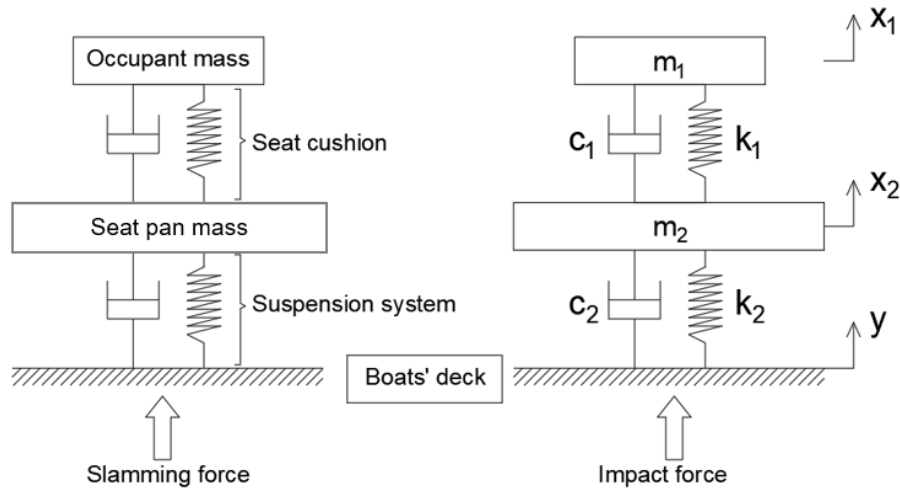


Fig. 7 Seat suspension system (two degrees of freedom)

For mass  $m_1$

$$m_1 \ddot{x}_1 = c_1(\dot{x}_2 - \dot{x}_1) + k_1(x_2 - x_1) \tag{1}$$

For mass  $m_2$

$$m_2 \ddot{x}_2 = -c_1(\dot{x}_2 - \dot{x}_1) - k_1(x_2 - x_1) + k_2(y - x_2) + c_2(\dot{y} - \dot{x}_2) \tag{2}$$

where

$m_1$  is the occupant's mass,

$m_2$  is the seat-pan mass,

$k_1$  is the stiffness of the seat's foam,

$k_2$  is the spring stiffness of the seat's shock absorber,

$c_1$  is the viscoelastic damping of the seat's foam,

$c_2$  is the viscous damping of the seats' shock absorber,

$x_1$  is the occupant mass absolute displacement,

$x_2$  is the seat-pan mass absolute displacement,

$y$  is the base absolute displacement.

#### 2.4 Instrumentation and drop test procedure

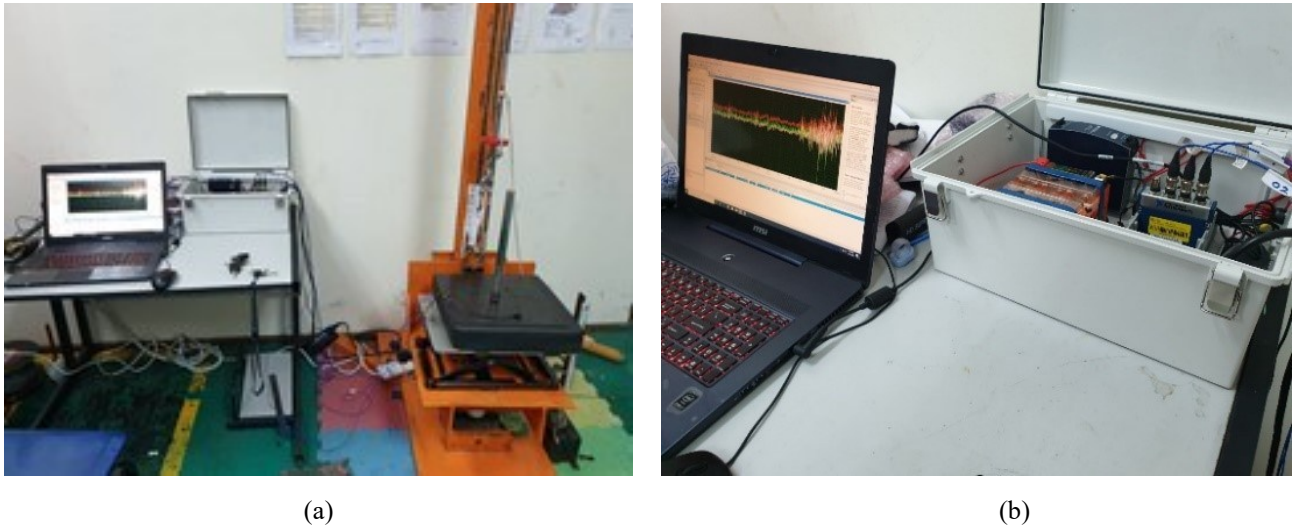
The drop test rig is equipped with three general-purpose accelerometers from the same model, PCB. All accelerometers are single-axis piezoelectric types, also known as Integral Electronics PiezoElectric (IEPE). Table 1 shows details on the accelerometers used for this test.

Table 1. General-purpose accelerometers used in the drop tests

	Accelerometer 1	Accelerometer 2	Accelerometer 3
Model	LW252929 PCB	LW254897 PCB	LW254897 PCB
Measurement location	On carriage base	On seat pan	On saddle plate
Measurement range	±500 g peak	±500 g peak	±500 g peak
Sensitivity	9.81 mV/g	9.87 mV/g	9.93 mV/g
Frequency range	0.5 to 10,000 Hz	0.5 to 10,000 Hz	1 to 10,000 Hz

A complete Data Acquisition System (DAQ) is composed of accelerometers, a signal conditioner module, a controller, and a personal laptop. The signals measured by the accelerometers are conditioned by a signal conditioner module specifically designed for vibration and noise (model number NI 9234) and the controller (model number cDAQ-9174). These signals are then interfaced, logged, processed, and analyzed

using the powerful LabView-2011 software. LabView-2011, developed by National Instruments, is instrumental in our data acquisition process, ensuring a 1kHz sampling rate. Fig. 8 illustrates the configuration of instrumentation applied to the drop tower and the DAQ system setup.



**Fig. 8** Photos showing (a) drop tower, (b) DAQ System, and LabView setup

The drop test experiments were conducted as follows. First, the suspension seat was secured on the base carriage. Load plates, which replaced the passenger’s weight on the seat cushion, were securely tightened on the saddle plate. The saddle was then strapped on the seat cushion using tie-down ratchet straps. The carriage was lifted to the desired drop height using the electric winch. It was then dropped freely by manually pulling the locking pin on a quick-release hook, which was used to hook up the lifting eyelet on the carriage to the winch cable. At this point, DAQ LabVIEW was activated in run mode to capture data before releasing the carriage.

Displacements of the carriage and seat pan were recorded via a video camera placed on a tripod, as shown in Fig. 9. The captured videos were set to slow mode, which will then be used to validate the displacement analyzed by LabVIEW.

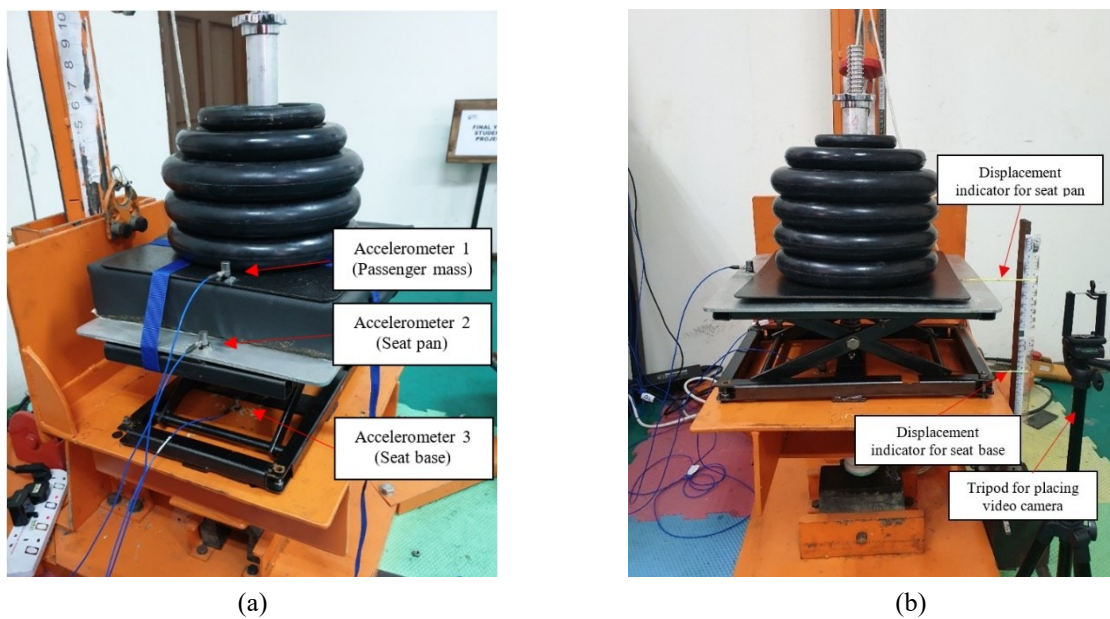


**Fig. 9** Photos showing (a) accelerometer setup and (b) displacement level indicator setup

### 2.5 Signal processing and impact acceleration theory

Acceleration signals received from accelerometers must be decomposed to extract impulse response signals when the carriage hits the soft rubber block installed on the foundation plate. Unnecessary signals from

small vibration amplitudes need to be filtered out from the data. These include vibrations created from the friction of bearings, the flexural response of the carriage, and vibrations caused when pulling out the locking pin on the quick-release hook.

Impulsive accelerations from drop tests can be evaluated by applying a low-pass filter to the acceleration data recorded by the DAQ. Filtering will remove high-frequency content that represents small vibration amplitudes. The Fast Fourier Transform (FFT) theorem determines the cut-off frequency for low-pass filtering.

Frequency domain representation shows the voltages at varying frequencies from the same signal. FFT graph spectrum will be plotted, and a suitable cut-off frequency can be examined and used in filtering [27]. Fig. 10 shows one of the examples of FFT spectrum analysis in which the input data has been taken from the drop test raw signals in this experiment. In this test, the Hanning window was chosen for FFT analysis due to its ability to reduce spectral leakage, resulting in a wide peak but low side lobe. The Hanning window also touches zero at both ends, eliminating all discontinuities compared to the Hamming window, which still has a slight discontinuity in the signal [28]. Spectral leakage comes from discontinuities or non-integer number of periods in a signal. In this experiment, the cut-off frequency is set at 20 Hz and filtered using a fourth-order low-pass Butterworth filter. Butterworth filter was chosen due to its maximum flat frequency response in the passband, used as an anti-aliasing filter, and suitable for motion analysis [29-32]. The exact cut-off frequency of 20 Hz has also been chosen by [15], 30 Hz frequency by [14], and 10 Hz frequency by [20]. All were based on their FFT spectrum analysis. International Maritime Organization (IMO) has also set the requirements for lifeboat drop testing for using a 20 Hz low-pass Butterworth filter for single shock impacts on water [33].

Research by Rosen et al. [34] concluded that a cut-off frequency of 30 Hz was suitable after assessing and combining simulated and experimental data. The data were obtained from extensive model experiments performed at the University of Naples "Federico II" (UNINA) and simulations performed at the Royal Institute of Technology (KTH), highlighting the collaborative nature of scientific research and the collective effort to advance our understanding in the field.

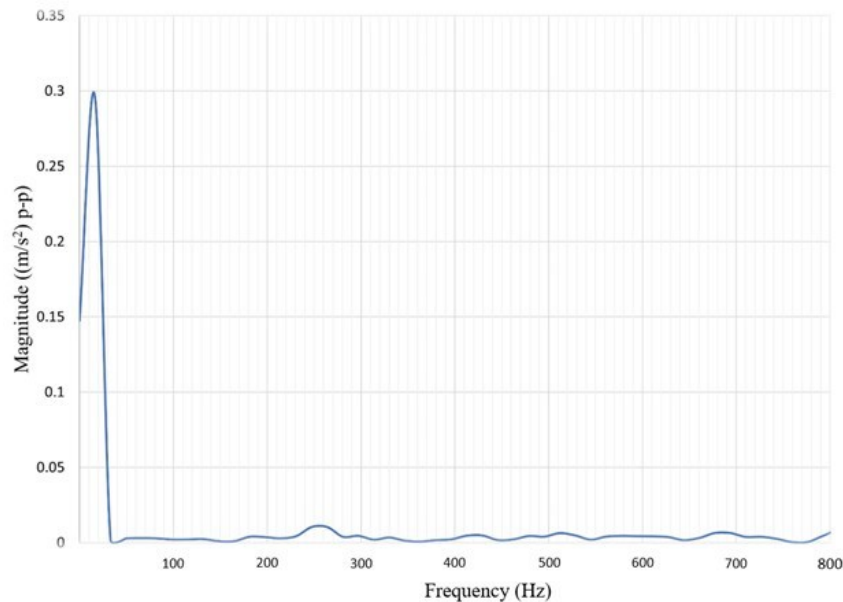


**Fig. 10** Analyzing FFT from one of the drop test raw data signals

Camilleri et al. [35] applied a 30 Hz cut-off frequency to assess slamming loads on HSC 9.5 m at full scale, a practical application of the research. After comparing the signals at several cut-off frequencies, Camilleri et al. [35] concluded that the 10 Hz cut-off frequency recommended by Riley et al. [27] is too low and does not accurately signify the peak acceleration rise. In a study conducted by Begovic et al. [36, 37] for model experiments conducted at UNINA, the cut-off frequency of 30 Hz was also chosen after observing extensive measured and simulated vertical acceleration results. According to Begovic et al. [36], the 30 Hz

cut-off frequency was found to be appropriate and not significantly affecting the rigid body dynamics, further emphasizing the practical relevance of the research.

In the sea trial experiment, for determining the slamming impact acceleration level to be used as an input acceleration on the seat base in this research, a 25 Hz cut-off frequency was found to be appropriate, which was also based on FFT graph spectrum analysis [24].

Average drop impact acceleration derived from Newton's second law is the time rate of change in velocity. Thus, acceleration during impact is given by Equation (3):

$$a = \frac{dv}{dt} = \frac{v_1}{\Delta T} = \frac{\sqrt{2gh}}{\Delta T} \tag{3}$$

where  $v_1$  is the dropping velocity before the impact,  $h$  is the drop height, and  $\Delta T$  is the pulse width of the impact. This is true when assuming inelastic impact. That is, rebound velocity is zero. In this experiment, for more accurate interpretation, rebound velocity must be considered. The impact acceleration is turned to Equation (4) after modeling the velocity output by applying a half-sine/cosine curve basis comparable to the pulse shape obtained from the accelerometers' response signal:

$$a_g = \sqrt{\frac{h}{2g} \frac{\pi(1 + \epsilon)}{\Delta T}} \tag{4}$$

where  $\epsilon$  is the coefficient of restitution that is given by Equation (5):

$$\epsilon = \frac{v_2}{v_1} = \frac{\sqrt{2gh_{rebound}}}{\sqrt{2gh_{compression}}} = \frac{\sqrt{h_{rebound}}}{\sqrt{h_{compression}}} \tag{5}$$

Equation (4) will be used to verify the base acceleration input obtained by accelerometers after the signal-filtering process.

### 2.6 Key parameters in suspension system

In vibrations and many experimental works, the logarithmic decrement method is fundamental knowledge used to evaluate an underdamped system's damping ratio in the time domain. Research conducted at Jiaotong University, Republic of China, has used the logarithmic method to analyze the damping coefficient for railway suspension systems [38] in their experimental analysis. Technical University-Sofia, Bulgaria, also used the same approach for the determination of the damping coefficient on rubber insulators [39]. Both studies have found that the method is efficient enough to extract this parameter despite having different types of damping properties, which are viscous and viscoelastic damping. Two oscillation systems with and without rubber insulators were used, and displacement time histories were compared for both systems to extract the damping ratio for rubber insulators.

The damping ratio can be calculated from its time history of oscillation in a single-degree-of-freedom (SDOF) system, as shown in Fig. 11. The motion of the system is decayed exponentially with its circular frequency of damped oscillation, where the undamped natural frequency, which is defined as, and is the damping ratio, is the stiffness coefficient, is the damping coefficient, is the critical damping coefficient, and represents the mass.

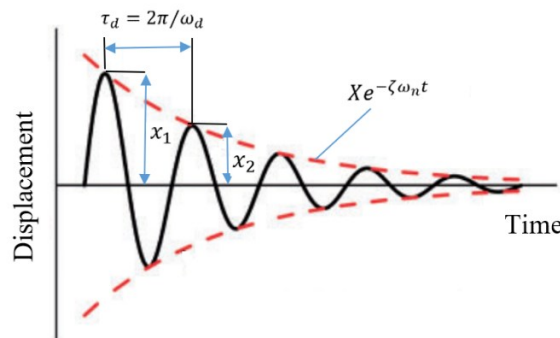


**Fig. 11** Displacement response for SDOF system for underdamped system

The system is underdamped when  $0 < \zeta < 1$ , and the body's motion is decayed with the factor of  $Xe^{-\zeta\omega_n t}$  with a damping period of oscillation given by  $\tau_d = 2\pi/\omega_d$ , as shown in Fig. 11. Two continuous amplitude  $x_1$  and  $x_2$  samples from peaks recorded in this oscillation data were collected and used for logarithmic analysis. The amplitudes of  $x_1$  and  $x_2$  are given by:

$$x_1 = Xe^{-\zeta\omega_n t}, x_2 = Xe^{-\zeta\omega_n(t+\tau_d)} \quad (6)$$

Logarithmic decrement  $\delta$ , is the ratio of any two consecutive amplitudes in Equation (7):

$$\delta = \ln\left(\frac{x_1}{x_2}\right) = \ln\left(\frac{Xe^{-\zeta\omega_n t}}{Xe^{-\zeta\omega_n(t+\tau_d)}}\right) = \zeta\omega_n\tau_d = \frac{2\pi\zeta}{\sqrt{1-\zeta^2}} \quad (7)$$

Thus, from Equation (7), logarithmic decrement is simplified to:

$$\delta = \frac{2\pi\zeta}{\sqrt{1-\zeta^2}} \quad (8)$$

Squaring the left and right of Equation (8) and taking the damping ratio as the subject yields:

$$\zeta = \frac{\sqrt{\delta^2}}{\sqrt{\delta^2 + 4\pi^2}} = \delta \sqrt{\frac{1}{\delta^2 + 4\pi^2}} \quad (9)$$

To analyze the spring constant  $k$ , the experiment applies Hooke's law theory. Hooke's law is written as,  $F = -k\Delta$  where  $\Delta$  is the distance of extension or compression of the spring. Here,  $F = W = mg$  where  $g$  is the gravitational acceleration.

Fig. 12 shows a simple experiment set-up to analyze the spring constant. In this test, the spring was positioned vertically under the seat pan, and the load plates were added 10 kg at a time. Each time the weight was added, the seat pan displacement, representing the spring compression, was recorded. The force versus spring displacement graph is then plotted, and the spring constant  $k$  (N/m) value is obtained from the graph's gradient.

**Fig. 12** Spring stiffness test

## 2.7 Dynamic response index (DRI)

P.R. Payne developed the Dynamic Response Index (DRI) in the 1970s under the U.S. Air Force to assess potential injury for humans in a seated position [13]. DRI was developed to predict the possibility of spine fracture injury during the ejection of the seat in an aircraft, and the model was based on years of collected Air Force ejection seat data. DRI is modeled as a human spine consisting of mass, spring, and damper of a single-degree-of-freedom system, representing maximum allowable compression on the human vertebral column. DRI was chosen in this research because it is calculated based on the largest peak of a singular event in a data set of vertical impact accelerations [18, 40-42]. Therefore, the most severe slam impact, which may

cause injury to the occupant’s spine, will be considered. DRI can be calculated using Equation (10) as below [43]:

$$DRI = \frac{\omega_n^2 \delta_{max}}{g} \tag{10}$$

where

$\delta_{max}$  is compression of the spine (compression of the spring),

$\omega_n^2$  is the square natural frequency of the spine modeled  $\omega_n = 52.9$  rad/s.

From the standard, the DRI value limit is set at 18, which corresponds to a 5 % probability of spinal injury rates [43], as shown in Fig. 13.

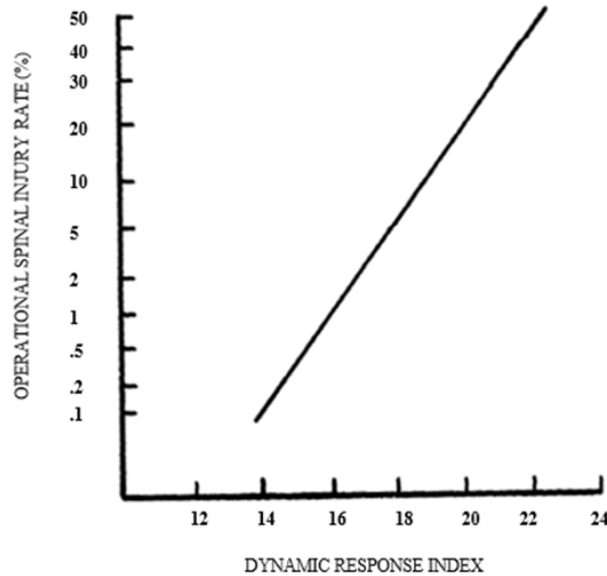


Fig. 13 Operational Spinal Injury Rate, as opposed to Dynamic Response Index (DRI), values [44]

### 3. Result and discussion

The results are divided into three sections. The first section discusses the result of base acceleration based on drop height, and the second section discusses the verification of the seat base displacement. Section three demonstrates the suspension seat's effectiveness in mitigating the slamming impacts onboard small HSC.

#### 3.1 Input base acceleration

As emphasized in part 2.5, the signal processing technique is pivotal when working with sensors such as accelerometers. The core lies in the meticulous selection of the cut-off frequency for the filtering process. A misjudged cut-off frequency choice could distort the amplitudes of the peak acceleration and lead to the loss of crucial physical data. The type of filter employed was less critical than the precision of the cut-off frequency value chosen for the filtering process. Butterworth, Bessel, and Kaiser window filters yield results with only a few percent differences [23]. In this experiment, a low-pass filter (LPF) was utilized to eliminate as many local structural vibrations as possible while retaining the maximum amount of rigid body vibrations data.

FFT analysis plays a crucial role in the study, as it can accurately indicate the vibration frequencies present in the time signals. However, a comprehensive validation process involving experimental and theoretical approaches is undertaken to ensure the filtering frequencies selected are accurate and reliable. This rigorous validation process bolsters the credibility of the results.

Table 2 Result of base acceleration theoretically and experimentally

Passenger weight (kg)	Drop height (mm)	Pulse width (ms)	Acc theory (m/s <sup>2</sup> )	Acc graph (m/s <sup>2</sup> )	Relative error (%)
-----------------------	------------------	------------------	--------------------------------	-------------------------------	--------------------

55	25	64	29.59	35.24	16.03
	50	79	41.80	45.77	8.67
	75	60	48.79	56.87	14.21
	100	69	59.26	64.51	8.14
	125	84	66.44	70.88	6.26
	150	56	72.79	77.40	5.96
60	25	64	29.53	33.75	12.50
	50	74	41.74	46.43	10.10
	75	61	51.24	58.41	12.28
	100	63	59.31	66.12	10.30
	125	80	66.41	71.65	7.31
	150	56	72.88	78.25	6.86
65	25	80	29.54	32.15	8.12
	50	80	41.83	41.71	0.29
	75	56	51.32	53.53	4.13
	100	66	59.44	61.61	3.52
	125	80	66.52	66.25	0.41
	150	54	72.73	73.42	0.94
70	25	86	29.49	30.42	3.06
	50	81	41.80	39.18	6.69
	75	55	51.45	50.92	1.04
	100	58	59.56	58.61	1.62
	125	56	66.68	65.20	2.27
	150	53	72.40	71.57	1.16
75	25	88	29.52	35.07	15.83
	50	79	41.82	42.58	1.78
	75	58	51.40	51.93	1.02
	100	57	59.60	59.91	0.52
	125	74	66.75	65.41	2.05
	150	54	72.67	70.43	3.18

Fig. 14 presents one of the results of the input base accelerations obtained during the experimental test versus theoretical calculation according to drop heights for a 65 kg passenger weight. For the theoretical calculation, the pulse duration is set to be at 70 ms. This value was selected based on the average pulse width from 30 drop test sets ranging from 53 ms to 88 ms, as shown in Table 2. The drop test impact event typically had a pulse duration of approximately 50 ms [44]. However, it depends on the material of the impacting surface, which can be changed according to its density, resilience, and thickness. Passenger weights were chosen from 55 kg to 75 kg with a 5 kg increase in the interval, and test height was from 25 mm to 150 mm with a 25 mm increase in the interval.

From the graph, the impact acceleration increased proportionally with the drop heights. Both experiments and theoretical results show good resemblance values with a low differentiation percentage. The selection of cut-off frequency for this filtering process is appropriate and acceptable. A comparison of base acceleration results calculated theoretically and experimentally for other passenger weights in Table 2 shows slight differences between calculation and experiment.

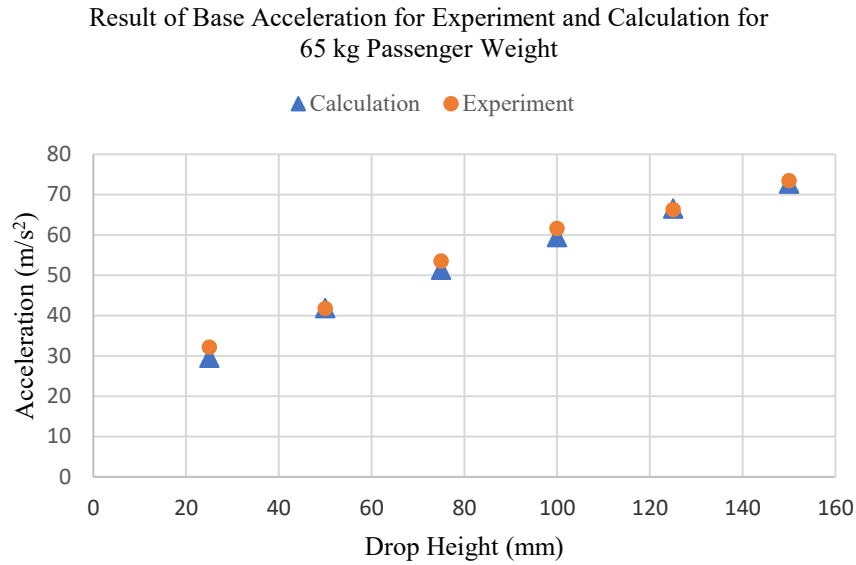


**Fig. 14** Base accelerations according to drop height

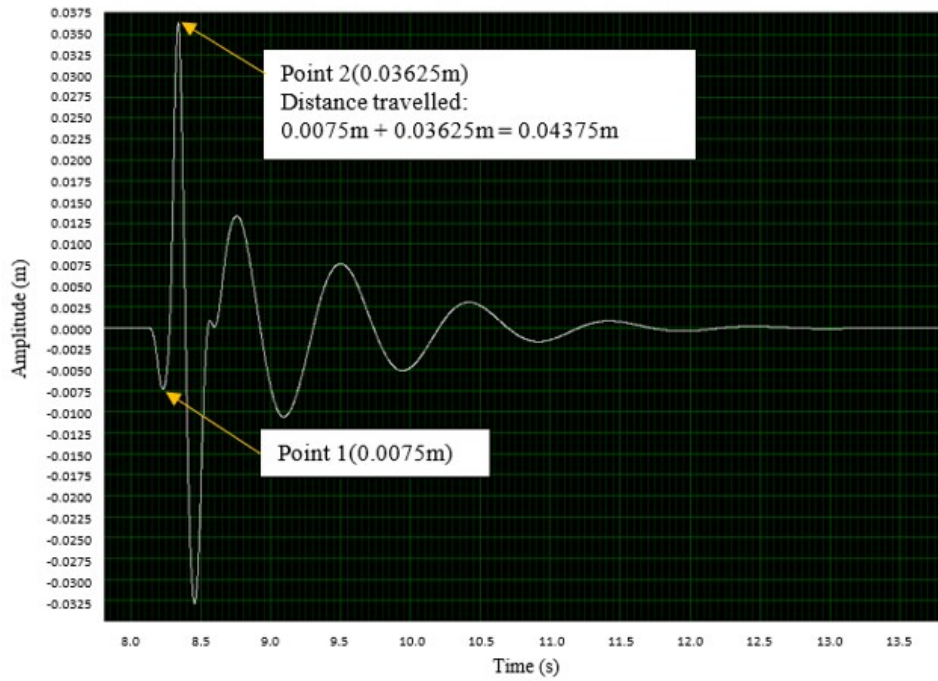
### 3.2 Validation of seat pan displacement

In this setup, the seat pan displacement was captured and analyzed through temporal image processing, allowing frame-by-frame analysis of motion over time to measure displacement accurately. A straight steel stick wrapped in green paper was attached to the seat pan to enhance visibility, as shown in Fig. 15. This stick was positioned very close to a measuring scale with a minimal 1mm gap to reduce parallax error. The camera, operating at 60 frames per second (fps) or 60 Hz, captured the motion of the seat pan as it impacted and rebounded from a rubber block.

**Table 3** Result comparison from graphs and recorded videos of seat pan displacement

Test height (m)	Displacement (m)		Dev (m)
	graph	camera	
25 mm	0.023	0.024	0.001
50 mm	0.035	0.031	0.004
75 mm	0.044	0.043	0.001
100 mm	0.050	0.050	0.000
125 mm	0.056	0.061	0.005
150 mm	0.060	0.068	0.008

The recorded footage was reviewed in slow motion to facilitate precise observation of the stick’s movement along the scale, making it easy to identify the seat pan’s maximum and minimum displacement points. The distance traveled throughout these points was taken and compared to the displacement time graph, as shown in Fig. 15. The sample results for seat pan displacement using 65 kg passenger weight are shown in Table 3. It can be seen from the table that both results from the graph and the actual distance recorded by the video camera are similar, with minimal differences in value. These minimal differences, while present, are within an acceptable range and do not significantly impact the overall accuracy of the results. The similarity of results shows the appropriate selection of filtering frequency and signal processing technique.



1<sup>st</sup> touchdown: point 1  
 Absolute time: 273.4ms  
 Reading on ruler: 0.046 m  
 Distance travelled: 0.089 – 0.046 = 0.043 m



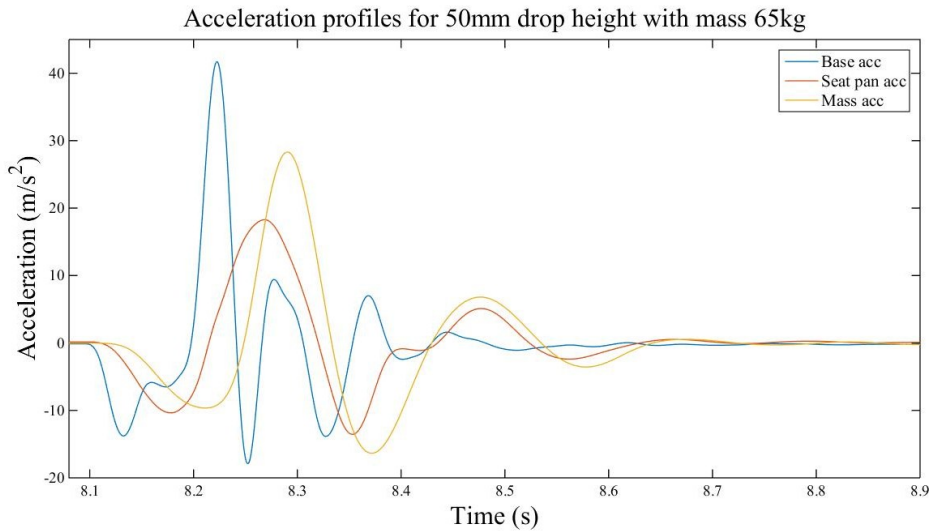
Maximum rise: point 2  
 Absolute time: 277.2 ms  
 Reading on ruler: 0.089 m

**Fig. 15** Comparison between graph and actual displacement of seat pan for 65 kg passenger weight for drop height 75 mm

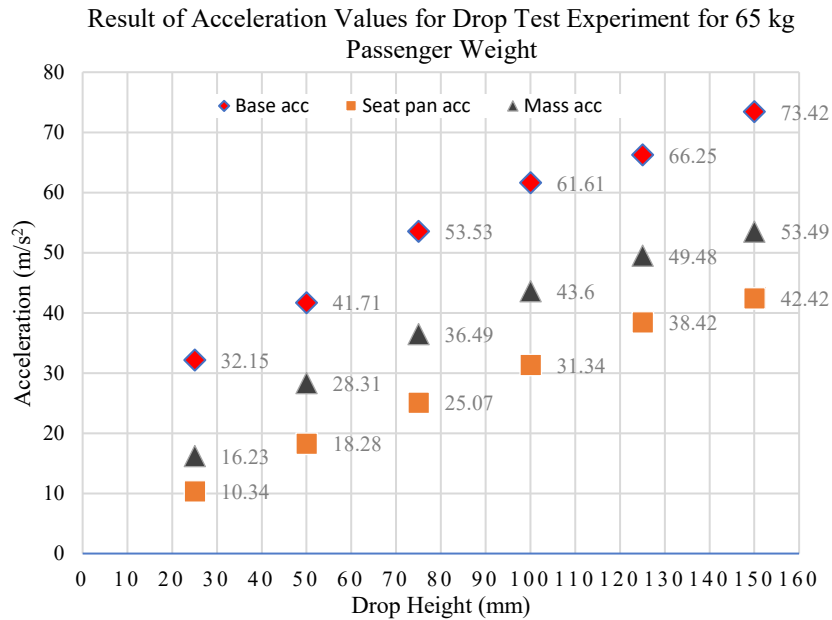
### 3.3 Seat effectiveness and safety

The seat effectiveness and safety standards used in this paper primarily focused on the seat's ability to mitigate the impact of slamming on occupants in the seated position. It is crucial to understand that the output results will indicate an occupant's probability of injury. Based on past research, the DRI standard is a suitable model for HSC to accommodate repetitive shocks due to slamming.

After the filtering process, a sample of absolute acceleration profiles obtained from a drop test for base carriage, seat pan, and mass is shown in Fig. 16. It can be seen that acceleration amplitudes for both seat pan and dummy mass are much lower than those for base acceleration. Moreover, the acceleration profiles of the seat pan and dummy mass have a wider pulse width and positive shifts in time compared to the base acceleration. These trends show that not only has the suspension seat reduced the number of accelerations on the occupant, but it has also successfully dissipated the impact energy and brought more comfort to the occupant, a reassuring aspect of its design. The acceleration magnitude for mass can be seen as higher than that for the seat pan. The higher amplitude can be due to the dummy mass losing contact with the seat cushion and slightly tilting during the impact. Observation from slow-motion video captured during the impact showed that the seat cushion has too low density and is easily squished, contributing to higher acceleration amplitude.



**Fig. 16** Sample of absolute acceleration profiles after LPF at 20Hz cut-off frequency



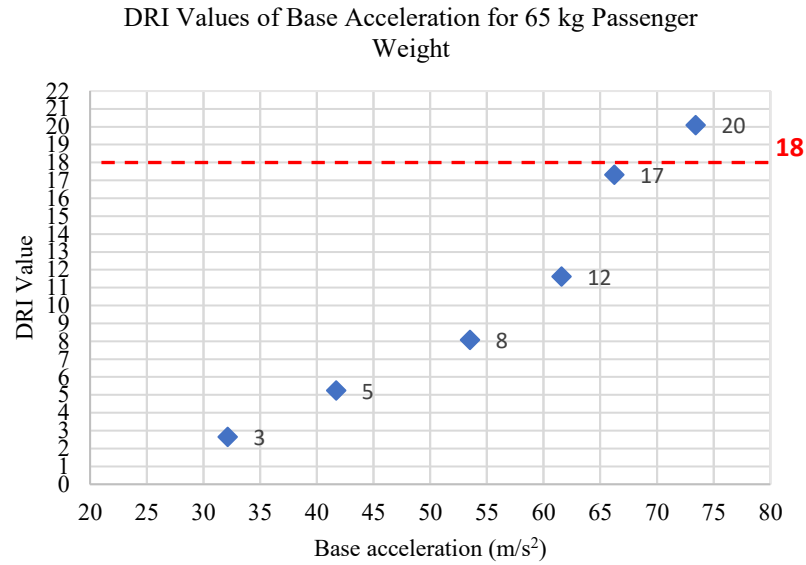
**Fig. 17** Peak accelerations as related to drop height for 65 kg passenger weight

Fig. 17 compares impact accelerations obtained for all three positions, i.e., seat base, seat pan, and mass acceleration. For all drop heights with the passenger's weight set to 65 kg, impact accelerations increase when the drop height increases. The seat could absorb impact accelerations at each drop height. Still, as can be seen clearly from the graph, the acceleration value recorded on the seat pan is proportional to the impact accelerations from the base. The behavior is valid for a passive suspension system with fixed damping properties. The trend is also similar for all tests with different passenger weights, as shown in Table 4.

Meanwhile, the seat successfully reduces impact accelerations from the seat base at each drop height. As conducted in this experiment, the DRI values remain a crucial standard criterion chosen in this research to prevent occupant injury. Fig. 18 illustrates the results of DRI values plotted against base accelerations, revealing that a DRI value under 18 is only possible if the base accelerations do not exceed 66 m/s<sup>2</sup> (6.73g). However, the graph also highlights a rapid increase in DRI values when the base acceleration value exceeds 54 m/s<sup>2</sup> (5.5g), thus indicating the lack of a damping coefficient to dissipate higher shock amplitude. The performance of the seat to mitigate the shock will decrease with an increase in impact accelerations, as seen in Fig. 19.

**Table 4** DRI value and percentage of impact reduction

Passenger Weight (kg)	Drop height (mm)	Seat base response		Seat pan response		Mass response		Impact reduction		DRI
		peak acc. (m/s <sup>2</sup> )	pulse width (ms)	peak acc. (m/s <sup>2</sup> )	pulse width (ms)	peak acc. (m/s <sup>2</sup> )	pulse width (ms)	seat pan (%)	mass (%)	
55	25	35.24	64	11.77	158	17.75	153	67	50	3
	50	45.77	79	18.44	173	28.82	158	60	37	5
	75	56.87	60	25.2	200	36.46	170	56	36	8
	100	64.51	69	31.45	212	43.68	197	51	32	12
	125	70.88	84	36.64	218	49.36	215	48	30	17
	150	77.4	56	40.17	224	52.99	231	48	32	20
60	25	33.75	64	10.58	165	17.23	155	69	49	3
	50	46.43	74	17.27	174	27.94	164	63	40	5
	75	58.41	61	21.38	196	34.19	183	63	41	8
	100	66.12	63	26.82	219	40.81	201	59	38	12
	125	71.65	80	32.61	227	47.65	221	54	34	17
	150	78.25	56	36.58	238	51.59	232	53	34	20
65	25	32.15	80	10.34	170	16.23	150	68	50	3
	50	41.71	80	18.28	175	28.31	160	56	32	5
	75	53.53	56	25.07	199	36.49	175	53	32	8
	100	61.61	66	31.34	214	43.6	192	49	29	12
	125	66.25	80	38.42	230	49.48	220	42	25	17
	150	73.42	54	42.42	241	53.49	228	42	27	20
70	25	30.42	86	10.84	165	15.78	156	64	48	3
	50	39.18	81	19.83	175	28.56	161	49	27	5
	75	50.92	55	27.58	201	36.77	175	46	28	8
	100	58.61	58	33.9	218	43.06	193	42	27	12
	125	65.2	56	40.09	232	47.62	211	39	27	15
	150	71.57	53	43.92	243	51.68	223	39	28	19
75	25	35.07	88	9.044	167	15.44	152	74	56	3
	50	42.58	79	15.26	176	27.41	169	64	36	6
	75	51.93	58	21.46	197	33.44	182	59	36	8
	100	59.91	57	28.09	214	41.13	201	53	31	12
	125	65.41	74	35.19	230	46.71	217	46	29	16
	150	70.43	54	41.11	244	50.67	229	42	28	19



**Fig. 18** DRI values as related to base accelerations

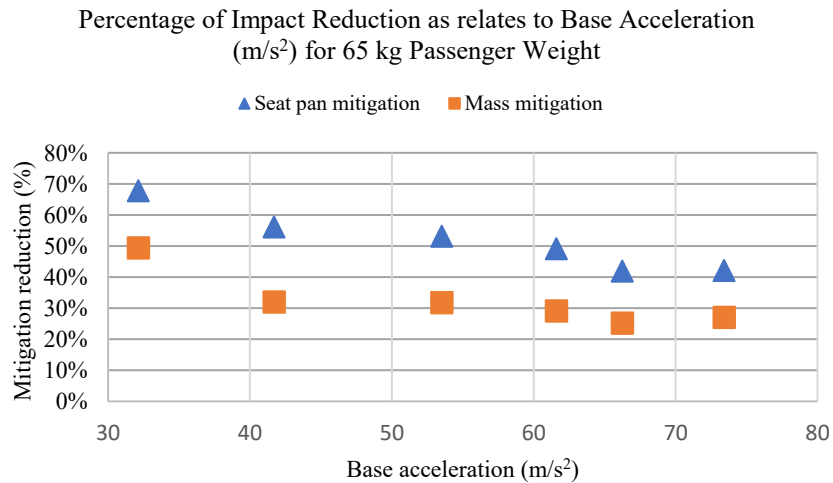


**Fig. 19** Impact reduction as relates to base acceleration

### 3.4 Modal parameter analysis

As discussed in part 2.6, this section will discuss the results obtained for the damping coefficient and spring stiffness possessed by the seat absorber. The seat uses an off-the-shelf shock absorber that is 125 mm in length from upper to lower eye mounts, is low-cost, and is a passive system shock absorber. Important parameters such as spring stiffness and damping coefficient were verified experimentally.

The damping coefficient was determined using the logarithmic decrement method, a widely accepted technique for extracting such characteristics. This method involves the use of two successive oscillation amplitudes of seat pan displacement, as illustrated in Fig. 20. The displacement profile was obtained by double integrating the acceleration data.

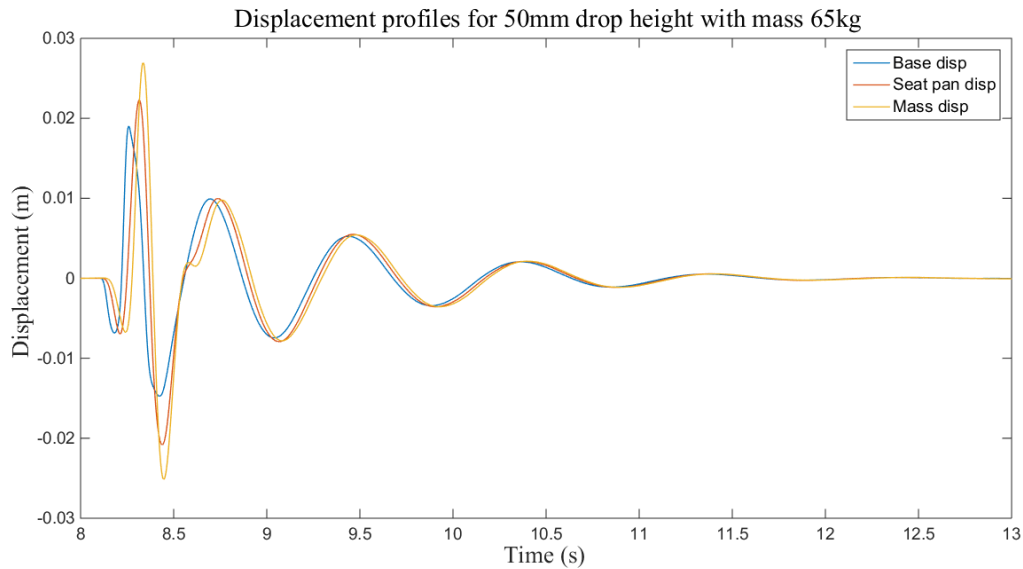


**Fig. 20** Absolute displacement profiles

From Fig. 20, two successive amplitudes and their damping periods were recorded. The process was repeated for each drop test that had been conducted. The graph shows that the motion is exponentially decayed, indicating the underdamped system with a damping ratio within  $0 < \zeta < 1$ . Information extracted from the graph was used to derive the damping coefficient using the logarithmic decrement method, and all results for each test are summarized in Table 5.

The average damping coefficient calculated from the table is 211 Ns/m. The suspension seat can be designed with a higher damping coefficient in the range of 500 – 832 Ns/m with a damping ratio of 0.3 to 0.5, as the average critical damping coefficient calculated from the table is 1664 Ns/m. Thus, the designed suspension seat can provide more comfort and safety. These values were chosen to avoid over-damping that will make the seat pan motion move too slowly and unable to absorb the following slamming impacts. The logarithmic decrement method becomes less and less precise as the damping ratio passes over the value of 0.5 [45]. A recent study by [46] has limited this value to 0.33 for optimum logarithmic decrement analysis. In this experiment, the average damping ratio is 0.13, and the value decreases as the drop heights increase. The value nearly reaches zero when the base impact is near 7g, which means the system has become undamped. This damping ratio is similar to that of a DRI value above 18, which indicates poor mitigation and safety characteristics.

Fig. 21 shows the spring stiffness graph plotted with a trendline for Hooke's experimental analysis at different loads, which have been added with a 10 kg mass one at a time. As can be seen, the slope of the graph represents the average spring stiffness value, which is 67685 N/m. This value is not far from the value stated in the product description, which is 64800 N/m. Generally, the force needed to compress or extend a spring by some distance is linear to that distance. The graph shows that, at the early stage of adding weight up to 30 kg, the compression distance deviates slightly from the trendline. This condition indicates that static friction exists on the seat structure and requires a weight of more than 30 kg to release the static friction force.

**Table 5** Modal parameters of suspension seat extract from logarithmic decrement method

Passenger Weight (kg)	Drop height, $h$ (mm)	Seat pan response						
		Damped period, $T_d$ (s)	Damped frequency, $\omega_d$ (rad/s)	Damping ratio, $\zeta$	Natural freq. $\omega_n$ (rad/s)	Critical damping, $C_c$ (Ns/m)	Damping coeff. $C$ (Ns/m)	Freq. ratio, $r$
55	25	0.40	15.52	0.14	15.66	1665	226	0.9907
	50	0.42	15.14	0.12	15.25	1621	188	0.9932
	75	0.42	14.96	0.11	15.06	1601	178	0.9938
	100	0.42	14.93	0.10	15.01	1596	165	0.9947
	125	0.42	14.89	0.10	14.96	1591	151	0.9955
	150	0.42	14.93	0.09	14.98	1593	138	0.9963
60	25	0.39	16.03	0.14	16.19	1721	239	0.9903
	50	0.41	15.22	0.12	15.32	1629	188	0.9933
	75	0.42	14.89	0.10	14.97	1592	165	0.9946
	100	0.43	14.68	0.10	14.76	1569	156	0.9950
	125	0.43	14.65	0.10	14.72	1565	152	0.9953
	150	0.43	14.72	0.09	14.78	1572	149	0.9955
65	25	0.39	16.11	0.14	16.28	1731	249	0.9896
	50	0.42	14.86	0.13	14.98	1593	202	0.9919
	75	0.43	14.75	0.12	14.86	1580	187	0.9930
	100	0.43	14.72	0.12	14.82	1576	184	0.9932
	125	0.43	14.61	0.12	14.71	1565	183	0.9932
	150	0.29	21.59	0.04	21.61	2298	95	0.9991
70	25	0.40	15.75	0.16	15.95	1696	265	0.9877
	50	0.43	14.79	0.14	14.93	1587	218	0.9905
	75	0.43	14.55	0.13	14.66	1559	196	0.9921
	100	0.44	14.38	0.13	14.50	1542	202	0.9914
	125	0.29	21.97	0.08	22.03	2343	176	0.9972
	150	0.29	21.37	0.04	21.39	2275	98	0.9991
75	25	0.39	15.95	0.14	16.12	1714	245	0.9897
	50	0.43	14.75	0.13	14.87	1581	199	0.9921
	75	0.44	14.41	0.12	14.52	1544	186	0.9927
	100	0.44	14.22	0.12	14.32	1523	184	0.9927
	125	0.29	21.67	0.07	21.73	2310	169	0.9973
	150	0.30	20.95	0.04	20.96	2229	91	0.9992

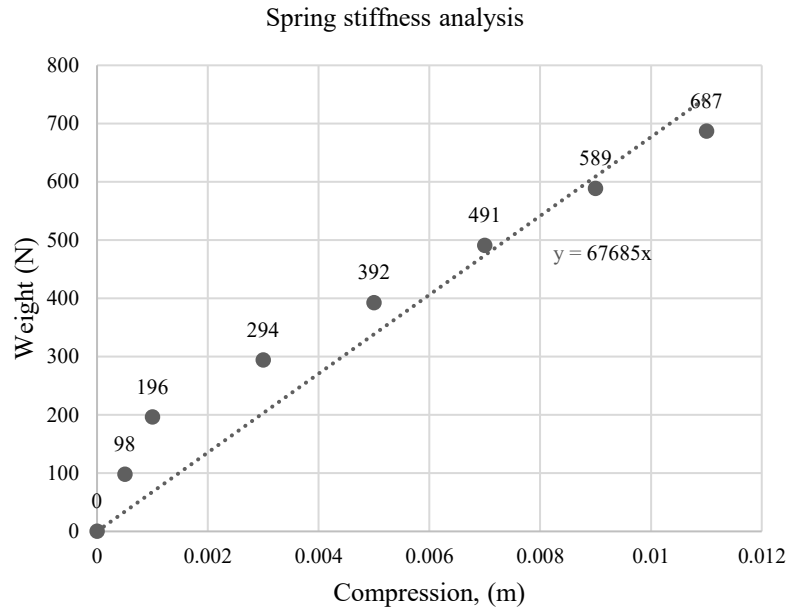


**Fig. 21** Graph of spring stiffness analysis

#### 4. Conclusion

This research assessed the effectiveness of the suspension seat, which was designed and fabricated to be operated on small high-speed passenger crafts. DRI results from the drop test experiment show that the seat could mitigate the slamming impacts on board HSC. DRI value limited to under 18 is achievable with base impact acceleration at 6.73g. The maximum deck impact acceleration value, recorded from previously conducted sea trials on 7.9 m HSC length in head seas conditions, is only 4.22g [24]. Thus, the result concludes that the seat has successfully demonstrated its effectiveness in mitigating the slamming impacts and is suitable to be installed onboard small high-speed passenger crafts. Modal parameters extracted from the displacement time graph using the logarithmic decrement method successfully determined the damping coefficient possessed by the seat absorber, that is 211 Ns/m, and Hooke's law experimental test had successfully confirmed that the seat absorber spring rate is at 64800 N/m as this value is very near to the experimental value of 67685 N/m. The spring rate value for this suspension seat is a bit bigger than that of other expensive suspension seats available on the market due to the short compression distance of the shock absorber. However, the damping value for the seat absorber used in this research can be increased to add more comfort and safety in the 550 Ns/m – 832 Ns/m range, with a damping ratio of 0.3 to 0.5. The inexpensive drop tower used in this experiment has successfully demonstrated its ability to simulate a single impact base acceleration. Using FFT to determine a suitable cut-off frequency for LPF, the signal processing technique has been validated theoretically by calculating the impact base acceleration and seat pan displacement by observing its motion from recorded video clips. For future work, the seat will undergo a sea trial test to analyze its performance in actual sea conditions. Innovation and enhancement of the designed seat can also be conducted in the future to produce a cost-effective suspension seat to be used on small HSCs.

#### ACKNOWLEDGEMENT

This research is supported by the Ministry of Higher Education (MOHE), Malaysia, under its Fundamental Research Grant Scheme (FRGS) number FRGS/1/2017/TK08/UTM/01/1.

#### REFERENCES

- [1] Jamison, D., Cannella, M., Pierce, E. C., Marcolongo, M. S., 2013. A comparison of the human lumbar intervertebral disc mechanical response to normal and impact loading conditions. *Journal of Biomechanical Engineering*, 135(9), 1-5. <https://doi.org/10.1115/1.4024828>
- [2] Kalkan, N., 2015. Human Factors and Ergonomic Considerations for Super Fast Boat Design. *Developments in*

- Environmental Science*, 10(9), 309-325.
- [3] Begovic, E., Bertorello, C., Pennino, S., Piscopo, V., Scamardella, A., 2015. Experimental assessment of comfort on board planing hulls. *Towards Green Marine Technology and Transport*. <https://doi.org/10.1201/b18855-65>
- [4] Pahensen, A., Garne, K., 2017. Adverse health effects and reduced work ability due to vertical accelerations in high performance marine craft personnel. in *Proceedings of the 16th International Ship Stability Workshop*, 5-7 June, Belgrade, Serbia, 103-108.
- [5] Wang, W., Du, H., Xiong, W., Nie, Y., 2023. Sensitivity Analysis and Optimization of the Hydraulic Interconnected Suspension Damping System of a Small Rescue Craft. *Journal of Marine Science and Engineering*, 11(10), 1-24. <https://doi.org/10.3390/jmse11101857>
- [6] Güzel, B., Korkmaz, F. C., 2020. Reducing water entry impact loads on marine structures by surface modification. *Brodogradnja*, 71(1), 1-18. <https://doi.org/10.21278/brod71101>
- [7] Jiao, J., Chen, Z., Xu, S., 2024. CFD-FEM simulation of water entry of aluminium flat stiffened plate structure considering the effects of hydroelasticity. *Brodogradnja*, 75(1), 1-28. <https://doi.org/10.21278/brod75108>
- [8] Trimulyono, A., Hakim, M. L., Ardhan, C., Ahmad, S. T. P., Tuswan, T., Santosa, A. W. B., 2023. Analysis of the double steps position effect on planing hull performances. *Brodogradnja*, 74(4), 41-72. <https://doi.org/10.21278/brod74403>
- [9] Jangam, S., Sahoo, P., 2021. Numerical investigation of interceptor effect on seakeeping behaviour of planing hull advancing in regular head waves. *Brodogradnja*, 72(2), 73-92. <https://doi.org/10.21278/brod72205>
- [10] MCA, 2008. International Code of Safety for High-Speed Craft. *Maritime and Coastguard Agency, International Maritime Organization (IMO)*.
- [11] Dobbins, T., Myers, S., Dyson, R., Gunston, T., King, S., Withey, R., 2008. High Speed Craft Motion Analysis - Impact Count Index (ICI). in *Proceedings of the 43rd UK Conference on Human responses to vibration*, 15-17 September, Leicester, UK, 15-17.
- [12] Garne, K., Burström, L., Kutteneuler, J., 2011. Measures of vibration exposure for a high-speed craft crew. *Proceedings of the Institution of Mechanical Engineers, Part M: Journal of Engineering for the Maritime Environment*, 225, 338-349. <https://doi.org/10.1177/1475090211418747>
- [13] U.S. Air Force, 1967. Sent System: Upward Ejection, Aircraft, General Specification for, MIL-S-9479B. *USAF*, 9479.
- [14] Gannon, L., 2017. Single impact testing of suspension seats for high-speed craft. *Ocean Engineering*, 141, 116-124. <https://doi.org/10.1016/j.oceaneng.2017.06.017>
- [15] Alam, Z., Afagh, F., Langlois, R., 2017. Efficient identification of naval high-speed craft shock mitigation seat modal parameters from drop-test data. *Journal of Dynamic Systems, Measurement, and Control*, 139, 1-10. <https://doi.org/10.1115/1.4035018>
- [16] Olausson, K., Garne, K., 2015. Prediction and evaluation of working conditions on high-speed craft using suspension seat modelling. *Proceedings of the Institution of Mechanical Engineers, Part M: Journal of Engineering for the Maritime Environment*, 229(3), 281-290. <https://doi.org/10.1177/1475090213515641>
- [17] Camilleri, J., Taunton, D. J., Temarel, P., 2018. Full-scale measurements of slamming loads and responses on high-speed planing craft in waves. *Journal of Fluids and Structures*, 81, 201-229. <https://doi.org/10.1016/j.jfluidstructs.2018.05.006>
- [18] Kearns, S. D., 2001. Analysis and mitigation of mechanical shock effects on high speed planing boats. Master Thesis, *Massachusetts Institute of Technology*, Cambridge, Massachusetts, United States.
- [19] SHOXS Website, 2020. Technical Data and Impact Science. <https://shoxs.com/impact-science> (Accessed Jul. 16, 2020).
- [20] Roberts, O. C., 2015. Development of the High Speed Craft Slam Impact Seat Test Rig. Master Thesis, *Carleton University Ottawa*, Ottawa, Ontario, Canada.
- [21] Zahid, M. S., 2022. Investigation of the Feasibility of Deploying Electro-rheological Dampers in a Drop Tower to Replicate the Impact Profiles of High Speed Craft. Master Thesis, *Carleton University Ottawa*, Ottawa, Ontario, Canada.
- [22] Riley, M. R., Haupt, K. D., Ganey, H. C. N., Coats, T. W., 2018. Laboratory test requirements for marine shock isolation seats. *Naval surface warfare center Carderock*.
- [23] Barber, J. D., 2016. Parametric investigation of a laboratory drop test to simulate base acceleration induced by wave impacts of high-speed planing craft. Master Thesis, *Old Dominion University*, Norfolk, Virginia, United States.
- [24] Abd Samad, F. I., Mohd Yusop, M. Y., Shaharuddin, N. M. R., Ismail, N., Bin Yaakob, O., 2021. Slamming Impact Accelerations Analysis on Small High Speed Passenger Crafts. *Brodogradnja*, 72(1), 79-94. <https://doi.org/10.21278/brod72104>
- [25] Littell, J., 2018. A summary of results from two full-scale fokker F28 vertical drop tests. *Langley Research Center*.
- [26] Liam, C., 2011. Testing and Modeling of Shock Mitigating Seats for High Speed Craft. Master Thesis, *Virginia Polytechnic Institute and State University*, Blacksburg, Virginia, United States.
- [27] Riley, M. R., Coats, T. W., Murphy, H., 2014. Acceleration response mode decomposition for quantifying wave impact load in high speed planing craft. *Naval surface warfare center Carderock*. <https://doi.org/10.21236/ADA621230>

- [28] National Instruments, A., Understanding FFTs and Windowing. *National Instruments*.
- [29] Ellis, G., 2012. Filters in Control Systems. *Elsevier Inc.* <https://doi.org/10.1016/B978-0-12-385920-4.00009-6>
- [30] Marshall, J., Coats, T., Riley, M., 2018. The rationale, assumptions, and criteria for laboratory test requirements for evaluating the mechanical shock attenuation performance of marine shock isolation seats. *Naval surface warfare center Carderock*.
- [31] Fouad, Y., 2014. An experimental methodology for characterizing high speed craft seat suspension components. Master Thesis, *Carleton University Ottawa*, Ottawa, Ontario, Canada.
- [32] El Tayeby, M., 2015. Modelling and synthesis of high speed craft acceleration profiles. Master Thesis, *Carleton University Ottawa*, Ottawa, Ontario, Canada.
- [33] IMO, 2003. Testing and Evaluation of Life-Saving Appliances, Maritime Safety Committee Resolution MSC.81(70), Life-Saving Appliances, 2003 Edition, International Maritime Organization.
- [34] Rosén, A., Begovic, E., Razola, M., Garne, K., 2017. High-speed craft dynamics in waves: challenges and opportunities related to the current safety philosophy. in *Proceedings of the 16th International Ship Stability Workshop*, 5-7 June, Belgrade, Serbia, 1-10.
- [35] Camilleri, J., Taunton, D. J., Temarel, P., 2018. Full-scale measurements of slamming loads and responses on high-speed planing craft in waves. *Journal of Fluids and Structures*, 81, 201-229. <https://doi.org/10.1016/j.jfluidstructs.2018.05.006>
- [36] Begovic, E., Bertorello, C., Bove, A., Garne, K., Lei, X., Persson, J., Petrone, G., Razola, M., Rosén, A., 2020. Experimental modelling of local structure responses for high-speed planing craft in waves. *Ocean Engineering*, 216, 1-13. <https://doi.org/10.1016/j.oceaneng.2020.107986>
- [37] Begovic, E., Bertorello, C., Pennino, S., Piscopo, V., Scamardella, A., 2016. Statistical analysis of planing hull motions and accelerations in irregular head sea. *Ocean Engineering*, 112, 253-264. <https://doi.org/10.1016/j.oceaneng.2015.12.012>
- [38] Shi, H. L., Wu, P. B., Luo, R., Zeng, J., 2014. Estimation of the damping effects of suspension systems on railway vehicles using wedge tests. *Proceedings of the Institution of Mechanical Engineers, Part F: Journal of Rail and Rapid Transit*, 1-15. <https://doi.org/10.1177/0954409714542861>
- [39] Kunchev, L. P., Georgiev, Z. A., 2019. Method for experimental determination of the coefficients of stiffness and damping of rubber insulators. *IOP Conference Series: Materials Science and Engineering*, 618(1), 1-7. <https://doi.org/10.1088/1757-899X/618/1/012057>
- [40] Alwis, P. De, 2014. Methods for Shock and Vibration Evaluation Applied on Offshore Power Boats. Master Thesis, *KTH Royal Institute of Technology*, Stockholm, Sweden.
- [41] Wice, A., 2015. Spatial dynamic modelling of high speed craft suspension seating. *Master Thesis, Carleton University Ottawa*.
- [42] Reynolds, D., Ayyad, E. A., Hachem, M., 2012. Evaluation of a pneumatic-seat-bladder-system designed for shock and vibration isolation. *University of Nevada*, Las Vegas
- [43] Destefano, L. A., 1972. Dynamic Response Index Minimization for Personnel Escape Systems. *Technical Report, DTIC Document*.
- [44] Alam, Z., 2013. Implementation of a drop test impact rig for dynamic testing of high speed craft shock mitigation seats and extraction of modal parameters. Master Thesis, *Carleton University Ottawa*, Ottawa, Ontario, Canada.
- [45] Inman, D. J., 2014. Engineering Vibration, Fourth Edition. *Pearson Education, Inc.*
- [46] Little, J. A., Mann, B. P., 2019. Optimizing logarithmic decrement damping estimation through uncertainty propagation. *Journal of Sound and Vibration*, 457, 368-376. <https://doi.org/10.1016/j.jsv.2019.05.040>